Predicted Transits of solar system objects

prepared by: F. Mignard
affiliation : OCA
reference: GAIA-C4-TN-OCA-FM-056-1
issue: 1
revision: 2
date: 2016-01-18
status: Issued

Abstract

Description of the software Predictor allowing to predict the passages in the Gaia FOVs for a list solar system sources over an interval of time defined by the users. The tech note gives the astronomical, instrumental and numerical principles applied to predict the transits of the sources and documents the file content for fixed or moving sources.

Document History

Issue	Revision	Date	Author	Comment
1	2	2016-01-08	FM	2 revision updated to agree with the latest changes done in code and output
1	1	2015-06-15	FM	1st revision updated to Predictor
1	0	2014-11-28	FM	First version issued to LL
D	0	2014-11-21	FM	Start of the document

Contents

Acronyms

The following table has been generated from the on-line Gaia acronym list:

Acronym	Description
AC	Across Scan
AL	Along Scan
CCD	Charge-Coupled Device
DPAC	Data Processing and Analysis Consortium
FOV	Field of View (also denoted FOV)
FPA	Focal Plane Assembly (Focal Plane Array)
GAREQ	GAia Relativistic Experiment on Quadrupole light deflection
GPDB	Gaia Parameter DataBase
IAU	International Astronomical Union
ICRF	International Celestial Reference Frame
ID	Identifier (Identification)
IDT	Initial Data Treatment
MOC	Mission Operations Centre
NSL	Nominal Scanning Law
OBMT	On-Board Mission Timeline
RA	Right Ascension
RMS	Root-Mean-Square
SM	Software Module
SRS	Scanning Reference System
TCB	Barycentric Coordinate Time
TDB	Barycentric Dynamical Time (obsolete)
VPU	Video Processing Unit

References

[AF-002], Fienga, A., Manche, H., Laskar, J., et al., 2013, *DPAC INPOP final release - INPOP10e*,
GAIA-CA-TN-IMC-AF-002,
URL http://www.rssd.esa.int/cs/livelink/open/3166347

[SK-018], Klioner, S., Mignard, F., 2014, *Recommended initial precession phase for Gaia Scanning Law*,
GAIA-C3-TN-TUD-SK-018,
URL http://www.rssd.esa.int/cs/livelink/open/3238429

[SK-022], Klioner, S., Mignard, F., 2014, *Recommended initial spin phase for Gaia Scanning Law for the period until 31.12.2015*,
GAIA-C3-TN-LO-SK-022,
URL http://www.rssd.esa.int/cs/livelink/open/3275314

[GAIA-FM-010], Mignard, F., 2001, *A practical scanning law for GAIA simulations*,
GAIA-FM-010,
URL http://www.rssd.esa.int/cs/livelink/open/358637

[GAIA-FM-017], Mignard, F., 2004, *The practical scanning law - an update*,
GAIA-FM-017,
URL http://www.rssd.esa.int/cs/livelink/open/356876

1 Introduction

A transit predictor has been developed within the CU4/SSO in order to be able to compute in advance the observations of solar system objects to be seen by Gaia during its operations. The software is an outgrowth of the simulator, based on similar overall principles, but aiming at accurate individual transit data instead of an overall statistical relevance which was the only requirement for the simulator. The simulator could work with an approximate sky, as long as it was representative of what Gaia would see in terms of observation density, magnitude distribution, etc., without intent of direct comparison on the sky for specific objects. In consequence in this earlier phase we did not need to pay extreme attention to the dynamical model (a 2-body Keplerian motion was acceptable) or to the full consistency of the orbital elements of the planets to their most up-to-date values. Our list was by definition our Universe model for the solar system. The simplified scanning law used by DPAC in the CU2 simulator was also sufficient (GAIA-FM-010,GAIA-FM-017) and provided the attitude model. The same liberty was used for the Gaia orbit about L2, with in fact nothing more real existing before launch.

Moving to a predictor of what actually happens during the actual mission implied a more rigorous modelling of the mission environment and of the dynamical modelling of the planetary motion. With the predictor the use of an exact Gaia scanning law is mandatory at any time to reproduce the actual pointing of each FOV. Similarly the Gaia orbit should be as close as possible to the true path of Gaia on its Lissajous orbit. Finally the orbital elements of the planets must be taken to full accuracy at a reference epoch and then the position and velocity must be propagated with planetary perturbations and numerical integration instead of the simplified 2-body problem.

2 Modelling

The program essentially solves for every planet the following equation in t for the ith planet and for each FOV f over an interval of time $[T_b, T_e]$,

$$\mathbf{G}_F(t) = \mathbf{U}_i(t) \tag{1}$$

where $\mathbf{U}_i(t)$ is the unit vector of the planet proper direction at time t and $\mathbf{G}_F(t)$ stands for the pointing direction of Gaia FOV F. The left-hand-side is the Gaia attitude model, here the NSL, while the right-hand-side resulted from the integration of the planetary motion.

The reference point in the FOV where the crossing is defined could be the center of the FOV or the SM gate center. (a global setting of the program). Over a certain interval of time the program finds all the roots $t_1, t_2, \cdots, t_{r_k}$ of Eq. 1. The solutions are found with an iterative process to locate a first approximation within a spin period and then accurately compute the solution with a Newton-Raphson method. The software has been very optimised for speed and allow to run a prediction for $\sim 500,000$ planets over 5 years in less than one hour of CPU on a desk-computer, including output files reaching 1GB. Testing and validations have been an important part of the development and took advantages of an implementation in Fortan and in Java running on two different environments. Comparison to actual Gaia observations of planets and stars have helped in the final debugging.

2.1 Input parameters

The transit predictor is based on the following general inputs :

- The osculating elements of the minor planets from the Astorb file maintained at Lowell Observatory `ftp.lowell.edu/pub/elgb/astorb.dat.gz`
- The Gaia scanning law (which is not exactly the attitude)
- The orbit of Gaia provided by MOC, regularly updated in the program environment
- The nominal description of the Gaia FPA giving the relative position of the CCDs and the nominal optical projection
- Time coverage between T_b and T_e.
- Range of magnitude in which detection are achievable, nominally $G < 21.5$

For each delivery these parameters become specific and the relevant specifications are included in the header of the file. For example a the delivery of June 2015 for the comparison to the true data one has the following:

- Osculating elements of about 650,000 planets from the Astorb file of June 2015. There are about 400,000 numbered planets (more than one opposition) and 250,000 provisionally labelled (lower orbit quality in general).
- Gaia scanning law (NSL) from 25 September 2014 onward defined by the two initial parameters on 1st September 2013, (i) initial precession phase = 52.66 deg, (ii) initial spin phase = 339 deg (SK-018, SK-022) and the spin rate 59.960499070315 ″/s TCB (from 59.96050 ″/s in TDB)
- The orbit of Gaia, provided by MOC. It includes the reconstructed orbit until the latest release and the targeted orbit afterwards. The targeted orbit is always within 7000 km of the actual orbit and generally much better.
- Start time : 25 September 2014, JD 2456925.5

- Duration: 460 days
- Faintest magnitude at SM detection G = 21.5

2.2 Dynamical model

The positions and velocity of the planets are computed by a numerical integration from the osculating epoch, using gravitational perturbations from the 8 planets (Mercury to Neptune) with the main component of the relativistic contribution.

The solar term with relativistic effect is computed as,

$$\frac{d\mathbf{v}}{dt} = -\frac{GM_{\odot}\,\mathbf{r}}{r^3} + \frac{GM_{\odot}}{c^2 r^3}\left(4GM_{\odot}\frac{\mathbf{r}}{r} - v^2\mathbf{r} + 4(\mathbf{r}\cdot\mathbf{v})\mathbf{v}\right) \tag{2}$$

with $\mathbf{r} = \mathbf{r}_p - \mathbf{r}_{\odot}$ for the heliocentric position vector of the planet

The planetary perturbations are given by,

$$\sum_k GM_k \left[\frac{\mathbf{r}_k - \mathbf{r}}{|\mathbf{r}_k - \mathbf{r}|^3} - \frac{\mathbf{r}_k}{r_k^3}\right] \tag{3}$$

where $\mathbf{r}_k$ is the heliocentric position vector of the kth planet. Solar System ephemeris are taken from INPOP10e) expressed in the barycentric frame with ICRF orientation and using TCB as independent variable (AF-002.

2.3 Instrument model

The general conventions regarding the FOVs and the local reference frame are shown in Fig. 3. The most important are the relative position of the FOVs in the across-scan direction, with a difference of 0.061 deg between the preceding and following FOVs, and the AL position of SM1/SM2 and AF1 last pixel where the transit times are actually computed. Pixel size, CCD positions are taken from the GPDB. Compared to initial simulation, in this version the position of AF1 reference pixel has been shifted by 2 arcsec (300 μm) to correct for a systematic difference in the crossing time of 0.03s seen with the ICRF sources.

2.4 Alignement to OGA1

The comparison of the transit times computed with the Nominal Scanning law to the observed ones for the ICRF sources displayed initially a systematic difference of 0.3s of time (different from the one mentioned just above), nearly constant from November 2014 to May 2015. Similarly I also noticed that the AC pixels at SM were systematically off by about 70 pixels in FOV1 and -50 pixels in FOV2, with scatter of about 10 pixels about the mean. This was due to the difference between the on-board attitude and the computed attitude derived from the NSL and basically this was not a surprise to see such a difference. But whereas a difference of 10 to 20 arcsec was expected, it was thought that it should be more or less random with variation of that amplitude changing with time. However this difference reduces in practice to a nearly constant rotation as shown in Fig. 1, giving the difference in the form of three infinitesimal rotations along the axes. There is one point every 10 mn during the period between January to October 2015. The scatter about the mean is limited to ± 2 arcsec and even less for the rotation about the z-axis.

This was a clear indication that most of the departure of OGA1 from NSL could be represented by a constant infinitesimal rotation, which was determined by straight comparison of OGA1 and NSL over several months. Having the two attitudes in the form of a rotation matrix, the infinitesimal rotation matrix is computed as,

$$\mathbf{R}_{\mathrm{I}} = \mathbf{R}_{\mathrm{OGA1}} \mathbf{R}_{\mathrm{NSL}}^{\mathrm{T}} \tag{4}$$

This rotation is implemented in the predictor as,

$$\mathbf{R}_{\mathrm{I}} = \begin{pmatrix} 1 & \gamma & -\beta \\ -\gamma & 1 & \alpha \\ \beta & -\alpha & 1 \end{pmatrix} \tag{5}$$

for the rotation to add to NSL to fit OGA1, with $\alpha = -14.75$ arcsec, $\beta = 1.7$ arcsec, $\gamma = 15.6$ arcsec. The latter value translates in the crossing time to $\frac{15.6}{60} \approx 0.27$s and corrected 90% of the systematic difference. A slight time variation is also included for γ with $\delta\gamma = -4 \times 10^{-4}\mathrm{day} + 2.62 \times 10^{-5}\mathrm{day}^2$ in arcsec and day the date in days from 01/07/2015. On the ICRF sources, whose positions are perfectly known in comparison to IDT accuracy, the predictions are accurate within 0.002 second. For the planets it is now limited by the orbit accuracy rather than the attitude and the prediction error is generally of the order of 0.005 s as shown in Fig. 2 based on the transits in June-July 2015 (100,000 transits). The flatness of the distribution is the result of the uncertainty in the computed position, which is typically between 0.1 - 0.2 arcsec, translating into 0.0015-0.003 s in the computed time. The overall shape comes from the difference between the true attitude and the approximated OGA1 in the software. I see no obvious explanation for the asymmetry and the more extended wing on the negative side.

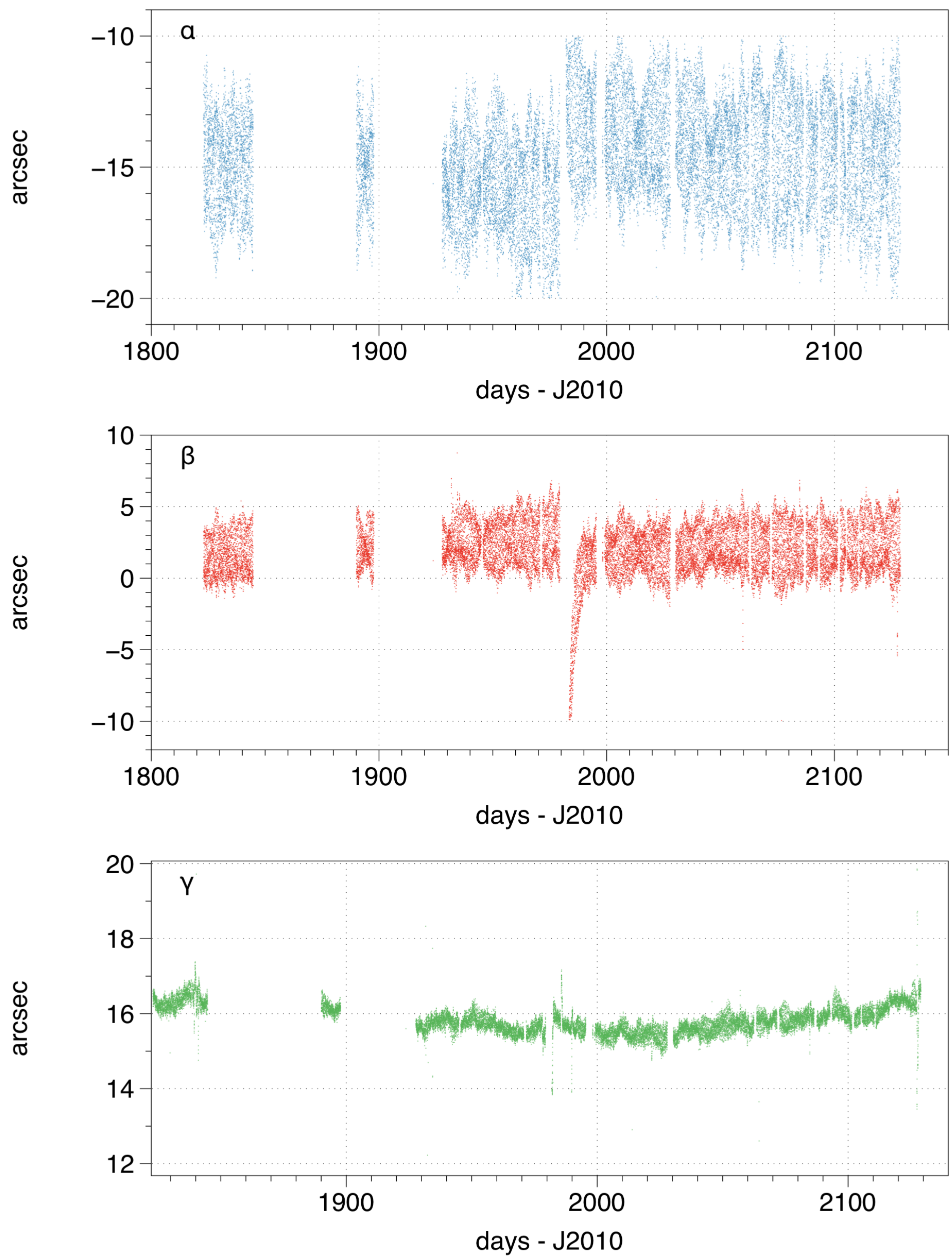

FIGURE 1: Difference between OGA1 attitude and the Gaia Nominal Scanning Law between January 2015 and October 2015. The difference is shown by the infinitesimal rotation angles in arcsec relating the two attitudes.

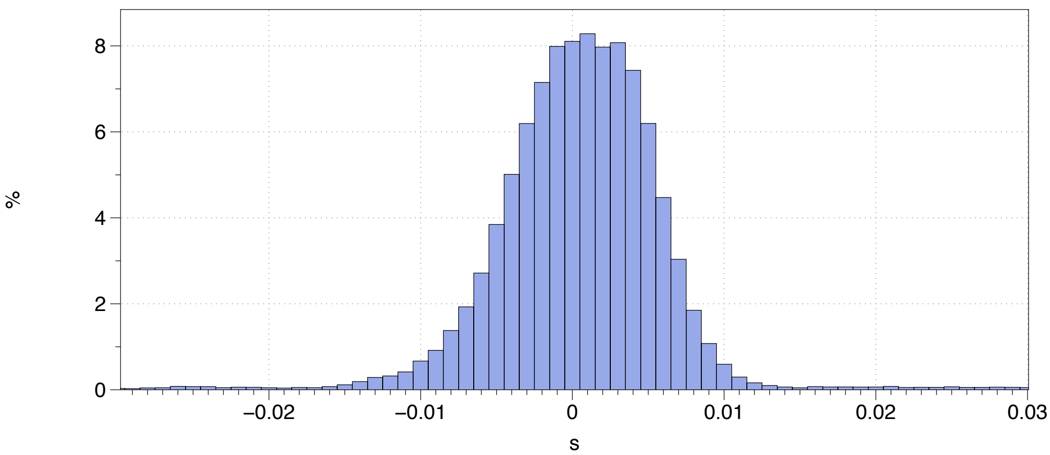

FIGURE 2: Difference between the observed and predicted transit times at AF1 reference pixel. The observed times are extracted from IDT data from June-July 2015 for the first 50,000 numbered planets and compared to the predicted values of the predictor software.

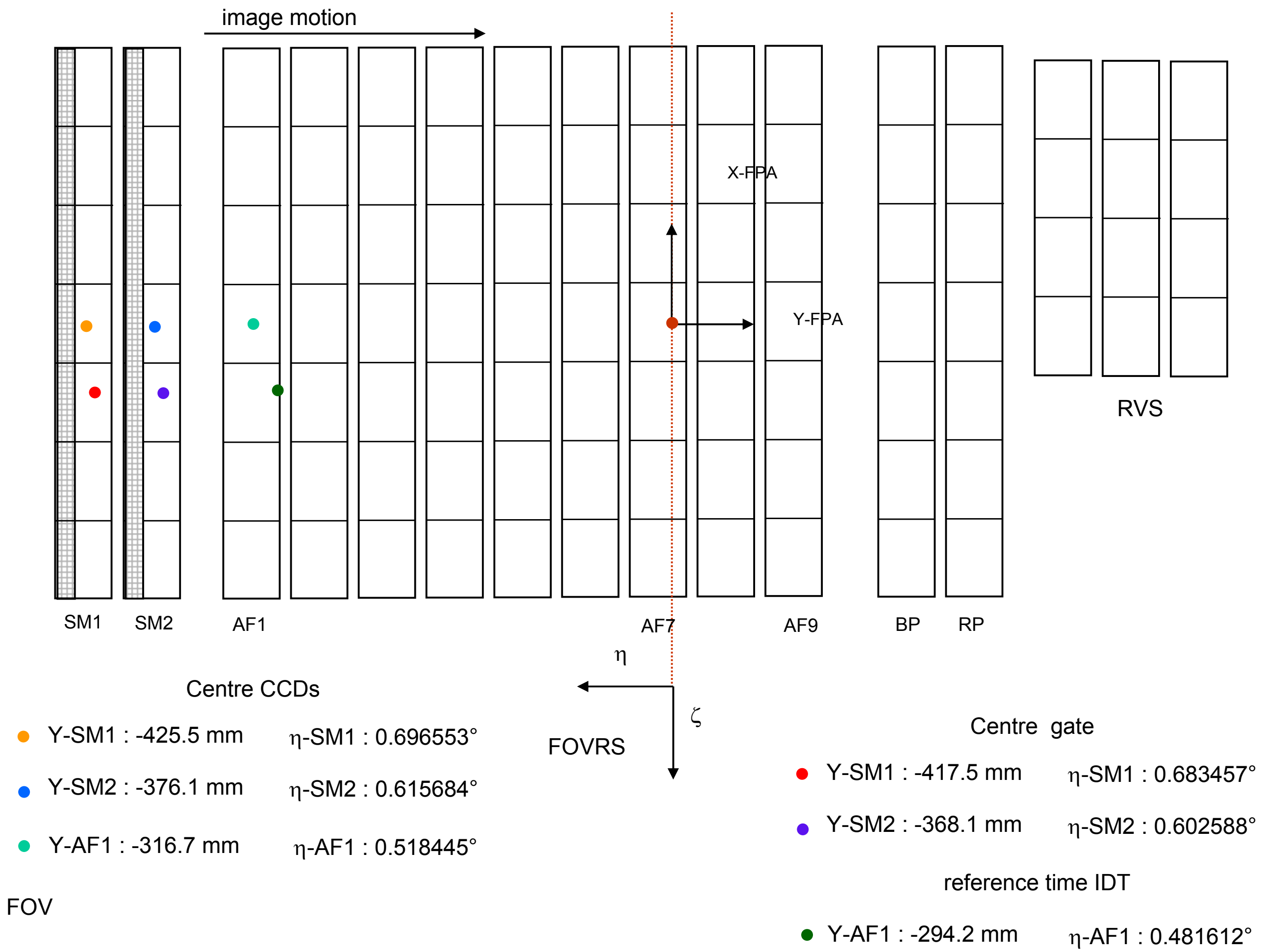

FIGURE 3: Conventions and reference frame used in the transit predictor to produce the list of transits. Crossing times are given at SM centre (where detection is done) and at AF1 last pixel to agree with IDT practice.

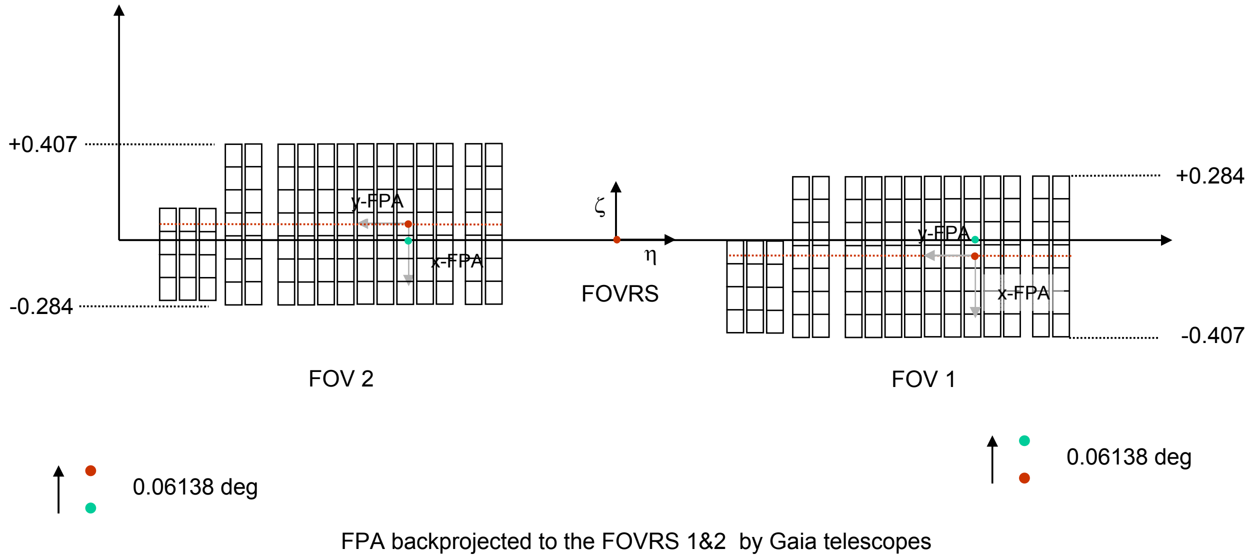

FIGURE 4: FOV settings used in the transit predictor.

3 Content of the delivery data

3.1 Field description for solar system objects

The standard output of the predictor comes as a single text file with one record per planetary transit. The file is sorted in increasing transit times in AF1 last pixel. Given the different interval of time between SM1-AF1 and SM2-AF1, it may happen that the records are not fully chronological when examined with the SM crossing time. The fields are described in Table 1 and further commented.

3.2 Additional comments on the entries

1 - This is the epoch coded (although in OBMT) in the TransitId by IDT. The records are sorted in increasing order of this field

2 - For provisional numbering, the ID may change with time until final numbering

4 - The G magnitude is estimated for a solar-like spectrum and using the Bowell 2-parameter expression to account for the surface scattering properties

8 – 11 - OBMT is computed from the TCB with a simple fit (slope, intercept) of the Gaia OBMT to TCB. The accuracy compared to the GaiaTools equivalent functions is better than 1 ms.

14 – 17 - This refers to the gaiacentric astrometric coordinates of the body when it is detected in SM. Coordinates are given in the ICRF frame. The transit epoch is determined with proper direction while for the astrometric coordinates the annual aberration has been removed. These coordinates are then directly comparable to stars'

20 – 21 - Inertial speed means that only the true motion of the planet is included. No contribution from the continuous change of the scanning plane.

22 This AC motion combines the inertial motion and the AC image displacement to the precession of Gaia spin axis.

23 - This is the angle between the direction of the celestial pole and that of the spin axis of Gaia. See Fig. 6.

24 - This is the heliotropic spin phase angle of the FOV at transit time.

3.3 Field description for stellar-like sources

A comparable software has also been developed for non moving source, like stars, galaxies, QSOs. Non moving means that the proper motions are not included in the astrometric modelling to compute the crossing time and the geometry of the crossing. This is in fact negligible

Field	Meaning	Comment
1	TCB of transit in AF1 last pixel	days from J2010
2	Planet ID	IAU final or provisional
3	FOV	1 : PFOV, 2 : FFOV
4	Estimated G magnitude	mag
5	Field coordinate ζ	degrees
6	VPU	1:7
7	AC coordinate in CCD strip	pixels
8	OBMT at detection in SM	days
9	OBMT at detection in SM	ns
10	OBMT of transit	days
11	OBMT of transit	ns
12	Calendar date of the transit epoch	TCB (same as field ♯1)
13	Calendar date of the transit epoch	UTC
14	astrometric right ascension at detection time	radians
15	astrometric declination at detection time	radians
16	astrometric right ascension at detection time	degrees
17	astrometric declination at detection time	degrees
18	motion in RA (with $\cos\delta$)	degrees/day
19	motion in Dec	degrees/day
20	inertial speed in the AL direction (η)	mas/s
21	inertial speed in the AC direction (ζ)	mas/s
22	time derivative of the AC field coordinate (ζ)	mas/s
23	position angle of the scan direction	degrees
24	nerby bright star flag	degrees
25	heliotropic angle of the planet at detection time	degrees

TABLE 1: Description of the file content for solar system objects

for the purpose of the predictor, and should it be introduced this would be very easy. The organisation of the software is very similar, and in fact simpler given the fact the celestial coordinates of the sources in the ICRF frame are read once for all and never recomputed. For the solar system objects the astrometry, attitude are in ecliptic frame while for the stellar sources the ICRF equatorial coordinates are used throughout.

For the stellar sources the output of the predictor comes as a single text file with one record per transit. The file is sorted in increasing transit times in AF1 last pixel. Given the different interval of time between SM1-AF1 and SM2-AF1, it may happen that the records are not fully chronological when examined with the SM crossing time. The fields are described in Table 2 and the comments for the solar system table apply when relevant.

Field	Meaning	Comment
1	TCB of transit in AF1 last pixel	days from J2010
2	Source record number in the input file	
3	Source ID	
4	FOV	1 : PFOV, 2 : FFOV
5	Estimated G magnitude	mag
6	Field coordinate ζ	degrees
7	VPU	1:7
8	AC coordinate in CCD strip	pixels
9	OBMT at detection in SM	days
10	OBMT at detection in SM	ns
11	OBMT of transit	days
12	OBMT of transit	ns
13	Calendar date of the transit epoch	TCB (same as field $\sharp$1)
14	Calendar date of the transit epoch	UTC
15	astrometric right ascension at detection time	radians
16	astrometric declination at detection time	radians
17	astrometric right ascension at detection time	degrees
18	astrometric declination at detection time	degrees
19	position angle of the scan direction	degrees
20	heliotropic angle of the planet at detection time	degrees

TABLE 2: Description of the file content for stellar-like sources

3.4 Accuracy

There are at least three sources of uncertainty to consider:

- The computational accuracy
- The position on the sky
- The position on the Gaia FPA and associated transit times

3.4.1 Computational accuracy

This refers to the numerical solution of the transit equation (Eq. 1) and to the numerical integration of the planetary dynamical equations, assuming every other parameters are exactly known. Convergence to the transit time is achieved to better that 1 ms during the Newton-Raphson iterations. Other computations have the accuracy permitted by the numerical representation of numbers, which, aside the epoch, is not a source of concern. The numerical integration of the planet motion over an interval of time that could reach 5 years is also compatible with a sub-mas astrometric accuracy. This is fully sufficient for the purpose of the transit predictor.

3.4.2 Celestial positions

The quality of the prediction of the gaiacentric position for solar system object is primarily determined by the knowledge of the osculating elements, rather than by the dynamical model, and by the predicted Gaia orbit. It is not easy to figure out how good the osculating elements are for every planet. As a rule of thumb for numbered planets (those with an IAU final number) the proper direction is generally better than 0.5 arcsec and often than 0.2 arcsec. For the provisional orbit of the recently discovered planets or those not re-observed after the first opposition, the uncertainty can range for sub-arcsec to something as large as 30 arcsec in exceptional cases. Based on the identification of moving bodies observed by Gaia and processed by CU4, many are in fact better than 2 arcsec.

For the stellar sources, the catalogue uncertainty depends very much on the source catalogue. While being negligible for the ICRF QSO's, in becomes larger for most of the SDSS QSOs or from older surveys and can reach several arcsec for the small catalogue of gravitational lenses. But even a 6 arcsec error will not produce an error in the crossing time larger tan 0.1 s.

The uncertainty stemming from the Gaia orbit itself can be easily estimated. There is a requirement that the actual Gaia orbit is always within 7000 km of the predicted orbit (this is in fact driven by the optimisation of the scanning law for the GAREQ experiment requiring the Gaia position to be known to better than 0.1 Jupiter radius). Assuming a planet at 2.5 au, this uncertainty in the Gaia barycentric position translates into nearly 4 arcsec for the planet Gaiacentric direction.

Comparisons of successive releases of the Gaia orbits indicate that the 7000 km requirement is largely met as shown in Fig. 5, where the ephemeris of two released orbits are compared. The first one released on Oct 2014, comprises the true orbit fitting up to this date and a predicted orbit after this date. The second orbit was provided on May 2015 and gives the actual orbit until this date. Therefore it is reasonable to consider that from May 2015 the uncertainty in the orbit used by the predictor is less than 2000 km, contributing no more than 1 arcsec in the uncertainty of the proper direction and much less if the RMS is used instead of the largest value. See also the IOW of 18 September 2015, Gaia orbit reconstruction.

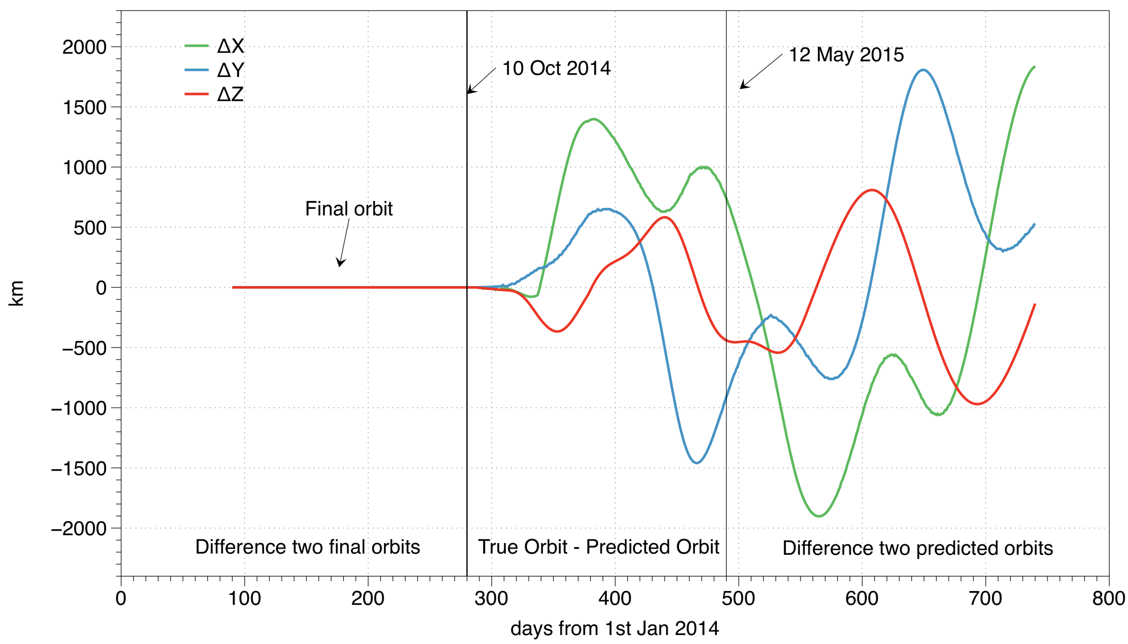

FIGURE 5: Difference between the MOC orbits provided on 14 October 2014 and 05 May 2015. Until 10 October 2014 we have the fitted orbits and the two are equal. Between October 2014 and May 2015, we have the comparison between a predicted orbit and an actual orbit, which shows a typical difference less than 2000 km which builds up rapidly after the start of the predicted orbit. The last segment compares two predicted orbits released at different epochs and the differences are similar.

3.4.3 Transit times and FOV coordinates

The predictor relies on the NSL (or EPSL when relevant) to predict the attitude of the spacecraft. As explained earlier in Sec. 2.4 it was possible to approach the true attitude (OGA1) by adding a single small rotation and this works well for 2015. Therefore the crossing time accuracy is now better than any known needs for this kind of prediction and the current limitation comes now from the orbit of the bodies. For the AC direction (ζ coordinate and AC pixel), the uncertainty resulting from the approximate attitude is within 10 AC pixels, or 2 arcsec on the FPA location. This is the location on the local frame, not on the sky, which is at least 10 times better than that in general.

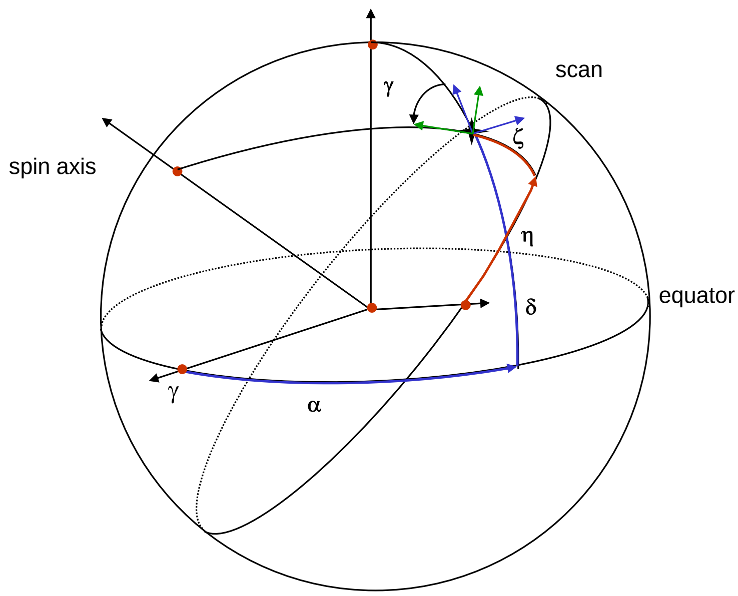

FIGURE 6: Conventions adopted in the field 23 of a transit record to orient the local SRS frame. The angle gives the orientation of the local η, ζ frame (the green one on the tangent plane) with respect to the equatorial local frame with α and δ (the blue one). The angle is between 0 and 360, positive and equal to about 45deg in the figure.